NEW METHODS FOR ASSESSING SPECTRAL, BI-DIRECTIONAL TRANSMISSION AND REFLECTION BY COMPLEX FENESTRATION SYSTEMS

Nicholas Gayeski
Marilyne Andersen, Ph.D.
Massachusetts Institute of Technology
77 Massachusetts Ave. Rm 5-418
Cambridge, MA, 02141
gayeski@mit.edu
mand@mit.edu

ABSTRACT

Advanced fenestration systems are increasingly being used to distribute solar radiation purposefully in buildings. Distribution of visible light and near infrared radiation can be optimized for daylighting and to reduce thermal loads. This can be achieved by fenestration systems that are spectrally and angularly selective. To study these systems, a device that measures the spectral, bi-directional transmission and reflection distribution functions of complex fenestration system components is under development. This device incorporates spectroradiometrically calibrated digital cameras and absorption filters to gather quasi-spectral information. The cameras could also be used to study the distribution of solar radiation in rooms.

1. INTRODUCTION

Efficient use of sustainable energy in buildings is a critical strategy for addressing global energy and environmental challenges. In the United States in 2006, building energy consumption accounted for 39 percent of total energy consumption. Excluding industrial buildings, 51 percent of building energy was associated with lighting, heating and cooling (1), all of which are greatly influenced by the thermal and optical properties of fenestration systems.

Intelligent use of solar energy, readily available for use in buildings, can meet or significantly offset many building energy loads. Fenestrations are an interface through which solar radiation can be gathered, distributed or rejected to optimize building energy performance. In the past fifty years, developments such as low emissivity and spectrally selective coatings have improved building energy performance through more effective control of solar gains. In addition, daylighting systems have been designed that redirect light deep into buildings to enhance lighting and reduce electrical energy needs. Some of these systems, such as profiled blinds, have an angular dependence and may, for example, reflect sunlight at high angles of incidence while redirecting light deep into a space at lower angles of incidence. Thorough analyses and descriptions of the many kinds of light redirecting daylighting systems can be found in other sources such as (2) and (3).

Angularly and spectrally selective fenestrations are one type of complex fenestration system (CFS) currently being researched. These systems can transmit or reflect different parts of the solar spectrum in different directions for different angles of incidence of solar radiation. The potential of this kind of system, for example, is to transmit visible light deeply into spaces throughout the year while reflecting near infrared radiation (NIR) during the summer and transmitting it towards thermal mass during the winter. As solar angles change throughout the year, the typical angles of incidence on different facades also change predictably and these systems could be tuned for optimal seasonal performance. One study showed that a spectrally and angularly selective coating could perform 18 percent better than a conventional spectrally selective coating (4), which simply reflects NIR throughout the year.

The ability to study the way these fenestration systems reflect and transmit solar radiation in different parts of the spectrum will help in characterizing, modeling and analyzing their performance in the built environment as well as designing new systems. Developing an innovative device to do this quickly, a spectral video-goniophotometer, should help advance the development, understanding, and implementation of advanced spectrally and angularly selective fenestrations.

2. GONIOPHOTOMETERS

Many goniophotometers have been built to study fenestrations, luminaires, and materials. Goniophotometers are devices that measure the transmitted or reflected luminance or radiance in a given direction relative to the incident illuminance or irradiance from a given direction onto a sample of interest (5). This information can be neatly summarized in a function called a Bi-directional Transmission (Reflection) Distribution Function (BT(R)DF). In general BT(R)DFs are dependent on two angles of incidence, two angles of reflection, wavelength and the polarization of source radiation (6). Mathematically, BT(R)DFs can be described as follows:

$$BT(R)DF_{e(l)}(\theta_{t(r)},\varphi_{t(r)},\theta_i,\varphi_i,\sigma,\lambda)=\frac{L_{e(l)}(\theta_{t(r)},\varphi_{t(r)},\theta_i,\varphi_i,\sigma,\lambda)}{E_{e(l)}(\theta_i,\varphi_i,\sigma,\lambda)}$$

$(\theta_{t(r)},\varphi_{t(r)})$ are the zenithal and azimuthal angles of transmission (reflection) of emerging radiation

(θ_i,φ_i) are the angles of incidence of incoming radiation

σ,λ are the polarization and wavelength of radiation

$L_{e(l)}$ is the radiance (luminance) of emerging radiation

$E_{e(l)}$ is the irradiance (illuminance) of incoming radiation

BT(R)DFs tell you the amount of irradiation (illumination) that gets redirected into a particular direction. Its units are per steradians, sr^{-1}. BT(R)DFs measured by goniophotometers are used to visualize the distribution of radiation emerging from a sample. They are also used to model the performance of systems through software such as Window5, DELight and Radiance. Most existing goniophotometers do not provide spectral or polarization information, but rather provide photometric or radiometric BT(R)DFs of a fenestration system for a particular type of spectrum, like daylight.

Goniophotometers can be divided into two categories, scanning and projection goniophotometers (5). A typical scanning goniophotometer consists of a light source, sample, and a detector which can be repositioned in some combination such that radiation reflected or transmitted in different directions can be measured by the detector for different angles of incidence of incoming radiation. The detector typically measure total luminance, radiance over a certain band or even spectral radiance in some devices (5). They are called scanning goniophotometers because they scan the hemisphere for reflected and transmitted radiation. Figure 1 shows a schematic of a recent device developed by pab™ optical consultancy (Germany) as an illustration of a state of the art scanning goniophotometer (7).

Two major drawbacks of scanning goniophotometers are the need for many measurements at many angles of reflection or transmission, which takes time, and discrete coverage of the hemisphere. More recently, projection-based goniophotometers have been developed using digital cameras that measure an entire hemisphere of transmission or reflection in one image. These devices typically project the full hemisphere of radiation transmitted or reflected by the sample onto a digital camera using diffusely or spectrally reflecting surfaces. A schematic of a projection based goniophotometer developed at École Polytechnique Fédérale de Lausanne (EPFL) is shown below which constructs a hemisphere from six images (8).

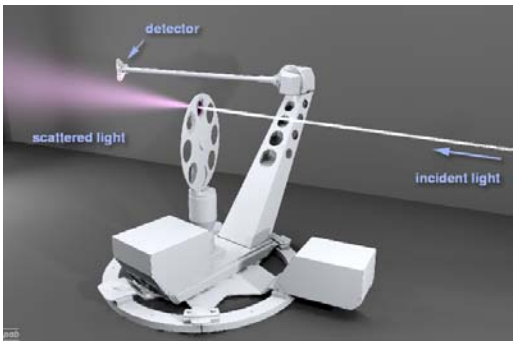

Fig. 1: pab-opto scanning goniophotometer schematic (7)

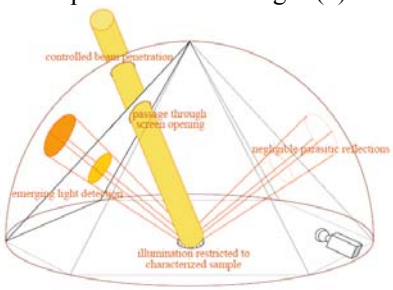

Fig. 2: EPFL projection goniophotometer schematic (8)

Projection goniophotometers have the advantages of being much faster than scanning goniophotometers and having continuous coverage of the entire hemisphere. However, unlike scanning goniophotometers they have the spectroradiometric limitations of digital cameras. Previous projection goniophotometers are limited to measuring total photometric BT(R)DFs. This is usually achieved by correcting the spectral response of a camera to match the photopic response of the human eye using appropriate filters for black and white or color cameras.

Some existing scanning goniophotometers have the ability to measure wavelength dependent bi-directional properties by using spectrometers or silicon and indium gallium arsenide (InGaAs) sensors as detectors. This enables the measurement of radiometric and photometric spectral BT(R)DF. None of the existing projection goniophotometers for fenestration systems can measure radiometric BT(R)DFs, nor can they provide information about the wavelength dependence of BT(R)DF (5). While

this is acceptable for measuring the daylighting performance of fenestrations, it does not provide the ability to study systems where thermal issues are of interest, nor does it provide information about spectrally selective components apart from their impact on total luminance distribution.

3. A SPECTRAL VIDEO-GONIOPHOTOMETER

A new goniophotometer is being developed at the Massachusetts Institute of Technology (MIT) that will merge the speed and continuous coverage of projection goniophotometers and spectral analysis capabilities of certain scanning goniophotometers. This is achieved through spectroradiometric calibration of a charge coupled device (CCD) and an Indium Gallium Arsenide (InGaAs) NIR digital camera used in conjunction with absorption filters.

The goniophotometer under development draws inspiration from a concept and a device built at the Lawrence Berkeley National Lab (6). Like a typical projection goniophotometer, it makes use of a light source, a rotating sample holder, a projecting device, and digital cameras. The light source is a 400W Dedolight HMI lamp chosen for its relative spectrum, which is similar to sunlight, and its collimation. A beam shaper is used to ensure the same spot size for different angles of incidence (9). Samples are mounted on a table with two degrees of rotational freedom to change the angles of incidence of light (10). To project light from the sample onto a camera, it is reflected off of an aluminum-coated, semi-transparent acrylic ellipsoid. Light can be transmitted through the semi-transparent ellipsoid to study reflection from a sample. The ellipsoid is positioned with the sample at one focal point and a digital camera at the other focal point. In this position, light reflected or transmitted by the sample will travel from one focal point to the other for recording by the camera. Pixel locations on the camera's image can be correlated to angles of incidence of incoming light, which can be correlated to angles of emergence from the sample (9). A schematic of the device is shown in Figure 3.

A photopic V(λ) filter could be applied to the CCD camera, as in other goniophotometers (5), in order to measure photometric BT(R)DFs. However, the goal of this device is to also measure the radiometric BT(R)DFs across the solar spectrum, as well as its spectral dependence, while still providing reasonably accurate photometric BT(R)DF. Rather than using V(λ) filters on the camera lens, absorption filters are used to sample incident light in bands over which the cameras output can still measure radiance across the band reliably. The obvious solution is to use narrow passband filters to sample the light and recreate a detailed spectral radiometric BT(R)DF from 380-1700 nm, the range over which the cameras are sensitive, then deduce photometric BT(R)DF. ….

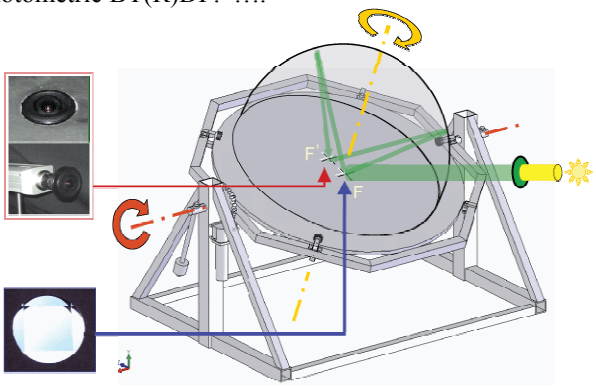

Fig. 3: MIT spectral video-goniophotometer schematic

The goal of this device, however, is *rapid* characterization of fenestration systems that provides useful, but not unnecessarily detailed information about wavelength dependence. To balance the need for speed and spectral analysis, the spectrum is sampled over larger wavebands, selected such that the total radiance and luminance across the band can still be measured accurately even for unknown spectra. The sections that follow will explain how these bands were chosen. Given that the total reflected or transmitted radiance or luminance over a set of bands can be predicted by the camera, a banded, spectral BT(R)DF can be constructed by comparing the radiance in each direction to the irradiance of the fenestration system.

The final output of this new spectral video-goniophotometer will be accurate photometric BT(R)DF and total radiometric BT(R)DF across a 380 to 1700 nm wave band. It will also provide reasonably accurate semi-spectral, i.e. banded, radiometric BT(R)DF across the same range. This is useful not only for predicting the angular distribution of luminance and radiance emerging from fenestration systems, but also for determining how much of different parts of the spectrum are directed in each direction. This will enable faster studies of fenestrations with spectrally and angularly dependent optical properties to provide additional information relevant to color rendering, the distribution of thermal gains and thermal comfort.

There were many steps involved in developing this spectral, video-goniophotometer. The rotating sample holder, beam shaper, and ellipsoid are described in previous works (9), (10). The remainder of the paper will describe the use of a Kappa DX20 color CCD camera as a spectroradiometer to measure spectral, BT(R)DF across 380 to 945 nm. This includes camera calibration, filter selection, reconstructing banded spectral reflectivity, and radiometric and photometric BT(R)DF error estimation. The spectroradiometric calibration of the InGaAs NIR camera, the spatial calibration of the cameras, corrections for the

spectral reflectivity and transmissivity of the half-mirrored ellipsoid and many other aspects of the device will be described in future papers.

4. SPECTRORADIOMETRIC CAMERA CALIBRATION

Spectroradiometric calibration of a digital camera consists of measuring the camera's digital response to known radiances of monochromatic light. The output of a digital camera for a given pixel at a given wavelength is related to the spectral exposure, in units of energy, of the sensor area correlating to that pixel. The spectral exposure is dependent on the number of photons of a given wavelength impinging on the detector area, which are in turn related to the radiance of the scene viewed by the camera (11). In its most simple form, the spectral exposure, H(λ) is related to scene radiance by:

$$H(\lambda) = k\frac{L_e(\lambda)}{N^2}t_{\text{int}}$$

where k is a constant depending on the optical and geometric properties of the imaging system, N is the aperture number, t_{int} is the integration time and $L_e(\lambda)$ is spectral radiance (12). In this application, the f-number of the lens is fixed at f/4, and thus the N in the above equation can be included in the constant of proportionality. Furthermore, the digital output for a pixel is physically related to the spectral exposure and can be thought of as a function of the scene radiance, such that:

$$NDL_{R,G,B}(\lambda) = DL_{R,G,B}/2^8 = f(H(\lambda))$$

where $NDL_{R,G,B}$ and $DL_{R,G,B}$ are the Normalized Digital Level and Digital Level of the R,G, or B channel.

4.1 Measuring the camera's non-linear response

To study the relationship between spectral exposure and NDL of the camera the camera output was measured against known monochromatic radiances and integration times, using the set-up described below. Rather than try to measure or estimate k, the constant of proportionality relating radiance to spectral exposure, the relationship between NDL and the product $L_e(\lambda)x\ t_{\text{int}}$ was measured directly. $L_e(\lambda)x\ t_{\text{in}}$ is a measure of the energy per unit area per steradian viewed by the camera. It is directly related to the real spectral exposure of the sensor area and will be referred to as $h(\lambda)$, because it is not strictly the spectral exposure of the CCD sensor. To verify the reciprocity relationship for digital cameras, the monochromatic radiance and integration time were both varied to show that the digital output of the cameras was related only to the product of the two, $h(\lambda)$ (12).

A Labsphere, KI-120 Illuminator tungsten-halogen light source, a Spectral Products CM110 monochromator, and a Labsphere Spectralon diffusing reflectance standard were used to create monochromatic radiances for viewing by the camera. The CCD camera is a Kappa DX20 color CCD camera with a Fujinon FE185C057HA high resolution fisheye lens and the NIR filter removed. The 8-bit digital output of the camera was averaged over the pixels viewing a monochromatic spot. The radiance viewed by the camera was estimated by measuring the irradiance of the diffusing reflectance standard and calculating the radiance reflected towards the camera. First, an Ocean Optics USB2000 spectrometer was used to measure the irradiance of the reflectance standard. A Labsphere integrating sphere was then used to repeat the experiments for more accurate irradiance measurements to confirm and refine the results of the spectrometer experiments, as well as to gather more accurate data for the absolute spectral responsivity calibration, described later. Figure 4 shows the typical S-shaped relationship between NDL and $h(\lambda)$ for the R, G and B channels.

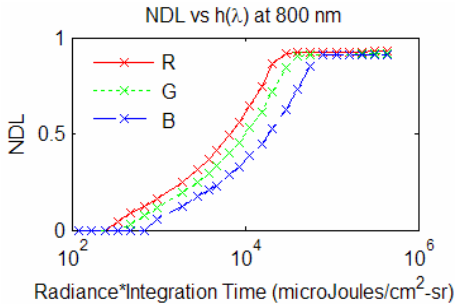

Fig. 4: R, G and B response to 800 nm radiation

The shape of these response curves was observed to be the same for each channel and all wavelengths. That is, for a given channel and wavelength, the ratio of one spectral exposure to another corresponds to a certain ratio of NDLs. These ratios are the same for different channels and different wavelengths. Therefore, if the spectral exposure for a certain channel and wavelength is normalized by the spectral exposure that leads to a selected NDL for that channel and wavelength, such as 0.3, the normalized response of the camera to the normalized spectral exposure is the same for any channel at any wavelength. Figure 5 shows all of the points for NDL and $h(\lambda)$ for all channels and wavelengths where the exposures $h(\lambda)$ have been normalized by the exposure resulting in NDL = 0.3 *(hence named* $h^{0.3}{}_{R,G,B}(\lambda)$), for each channel and wavelength, excluding points at saturation or below the threshold of the camera.

The response of a CCD camera is best approximated by certain functions, such as logistic dose response, sigmoid, asymmetric sigmoid, gaussian cumulative, and weibull cumulative functions (12). A logistic dose response function

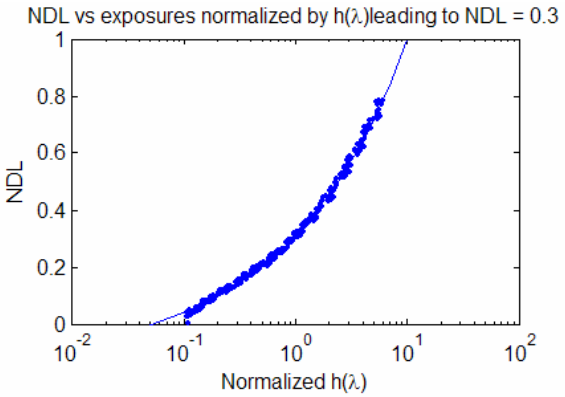

Fig. 5: Normalized response for R, G and B channels to many wavelengths fit with a logistic dose response function

was found to fit the Kappa DX20 response curve best over the range of NDL = 0.05 to 0.8. This curve is the solid line in Figure 5. All of the spectral sensitivity properties of the camera are contained in the wavelength dependent normalization function, $h^{0.3}_{R,G,B}(\lambda)$, for each channel. This function is:

$$NDL_{R,G,B} = a + \frac{b}{1+\left(\frac{h(\lambda)/h^{0.3}_{R,G,B}(\lambda)}{c}\right)^{d}}$$

For the Kappa DX20 CCD camera mounted with the fisheye lens and disregarding saturation and threshold points, the constants of the logistic dose response function were found to be: a = -0.13254, b = 363.51, c = 1.4468e7 and d = -0.40717.

4.2 Measuring spectral sensitivity

The spectral sensitivity of the camera, represented by $h^{0.3}_{R,G,B}(\lambda)$, was measured experimentally by comparing the normalized digital response of each channel to monochromatic radiances viewed by the camera for known integration times. The Ocean Optics spectrometer was used to measure the irradiance on a reflectance standard viewed by the camera at 5 nm intervals. The radiance viewed by the camera was calculated based on the measured irradiance and the reflectance standard's spectral properties. The ratio of the cameras actual NDL for a given radiance to an arbitrary normalization NDL, such as 0.3, can be correlated to the ratio of the actual scene radiance to the radiance that would lead to NDL = 0.3 using the logistic dose response function. In this way, the spectral exposures for different wavelengths leading to the same digital output for a given channel can be compared. Plotting the inverse of these normalized spectral exposures gives the absolute spectral responsivity (ASR) $r_{R,G,B}(\lambda) = 1/h^{0.3}_{R,G,B}(\lambda)$, in NDL/(μJ/cm^2–sr) (13), of each channel as shown in Figure 6.

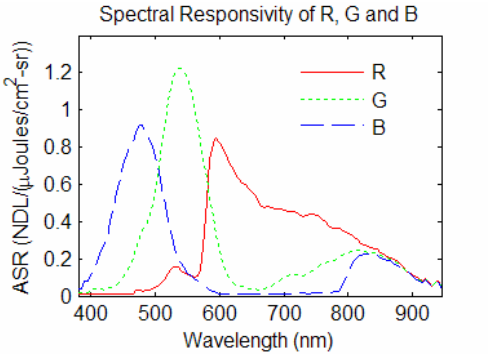

Fig. 6: Absolute spectral responsivity of the R, G and B channels

Inverting the logistic dose response function and factoring out a known integration time leads to a relationship between each channels digital output and the monochromatic radiance of the scene.

$$L_e(\lambda) = \frac{h^{0.3}_{R,G,B}(\lambda)}{t_{\text{int}}} \times c\left(\frac{b}{(NDL_{R,G,B}-a)}-1\right)^{1/d}$$

If narrow passband filters were used to isolate wavelengths in 5 nm bands the exact spectral, bi-directional reflection and transmission by samples could be measured. However, due to the desire for fast BT(R)DF assessment, filter cost and availability limitations, and the need for radiances above the camera's threshold, compromises had to be made to accommodate larger filter bands.

4.3 Measuring the response to polychromatic beams

In order to allow for larger spectral bands while still being able to correlate digital output to radiances, the response of the camera to polychromatic beams must be understood. Theoretically, the digital output of the camera to polychromatic beams should be related to the total, not spectral exposure (13). As a function of radiance, integration time, and ASR this can be written:

$$NDL_{R,G,B} = f\left(\int r_{R,G,B}(\lambda)h(\lambda)d\lambda\right)$$

If the total radiance of the beam across the spectrum to which the camera is sensitive is given by:

$$L_{e,beam,380-945} = \sum_{380-945} p_{\Delta\lambda} L_{e,beam,380-945}$$

where $p_{\Delta\lambda}$ is the fraction of the total radiance from 380 to 945 nm in a 5 nm band Δλ, then the equation above can be rewritten in discrete form as:

$$NDL_{R,G,B} = f\left(L_{e,beam,380-945} t_{\text{int}} \sum_{380-945} r_{\Delta\lambda} p_{\Delta\lambda}\right)$$

This says that the absolute responsivity of the camera to a polychromatic beam is simply a weighted sum of the absolute spectral responsivities, where the weights are determined by the relative spectra of the beam across the

waveband to which the camera is sensitive. For the Kappa CCD camera this region is 380 to 945 nm. For this work, the spectra must be aggregated into 5 nm bands because this is the resolution with which $r_{\Delta\lambda}$ was measured. The $r_{\Delta\lambda}$'s in the above equation are different for each channel and given by $1/h^{0.3}_{R,G,B,\Delta\lambda}$. Because the non-linear response of the camera has the same shape for all channels and all wavelengths, it is reasonable to assume that the function relating NDL and radiance for a polychromatic beam is the same as that for a monochromatic beam, and is given by:

$$NDL_{R,G,B,beam} = a + \frac{b}{1+\left(\frac{(L_{e,beam}t_{\text{int}})/h^{0.3}_{R,G,B,beam}}{c}\right)^{d}}$$

Where $1/h^{0.3}_{R,G,B,beam}$ is the absolute responsivity of the camera to the beam, which, from the equation above is:

$$\frac{1}{h^{0.3}_{R,G,B,beam}} = \sum_{\Delta\lambda}\frac{p_{\Delta\lambda}}{h^{0.3}_{R,G,B,\Delta\lambda}}$$

If the relative spectrum of the beam is known, then the equation for NDL can be inverted to solve for the radiance in the beam. The CCD camera can then be used as a multi-point radiance or luminance meter for polychromatic beams of known relative spectra across the 380 to 945 waveband. In controlled situations, such as a room with spectrally neutral surfaces and daylight or sunlight of known spectra, quick light distribution assessments can be made at locations of interest in the room for a large field of view.

To verify that the ASR calibration of the camera predicted the total radiance of polychromatic beams accurately, a series of pictures were taken with the Kappa CCD camera of a spot on the diffusing reflectance standard with a known spectrum. The spectral irradiance of the beam incident on the reflectance standard was measured using the spectrometer and integrated over 380 to 945 nm to calculate the total radiance seen by the camera in that waveband. Using the relative spectrum, the digital output of each channel was used to estimate the radiance of the beam. Figure 7 shows the NDL of each channel plotted against the measured exposure to the beam from 380 to 945 and the predicted exposures for those same NDL. The relative spectrum of the spot studied is also shown.

The measured and predicted exposures are seen to follow the same response curve very closely. Over a series of validation spots that included broadband spectra and monochromatic spectra, the average error for estimating radiance for each channel was found to be 8.9 percent for R, 4.3 percent for G, and 5.2 percent for B. This does not include behavior near saturation or spots to which a given channel was very insensitive. These calibration errors are a good estimate of the total errors in modeling the non-linear response of the camera and in the spectral sensitivity calibration.

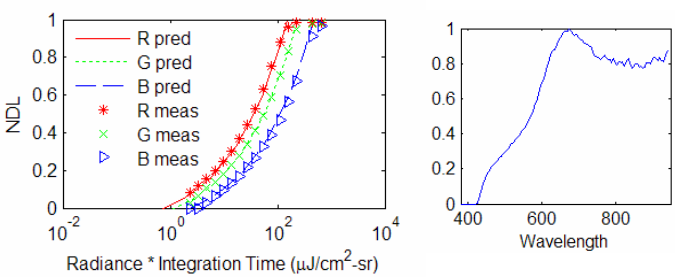

Fig. 7: Predicted versus measured exposures for one validation spot for each channel

4.4 Estimating banded spectral reflection or transmission for fenestration systems with unknown spectral properties

Measuring the radiance of beams with known relative spectra can be useful in many instances, such as measuring the BT(R)DFs of spectrally neutral fenestration systems or in studying radiance and luminance distribution in spaces where spectra are known. However, to study fenestrations with unknown, spectral BT(R)DF, it is important to be able to use the camera as a radiance and luminance meter even when the spectrum is unknown. Spectrally selective materials will change the spectrum of reflected or transmitted light, and thus change the absolute responsivity of the camera to the beam. The easiest way to address this issue, as mentioned before, is to use narrow passband filters to sample the spectrum, but this is prohibitive of quick analyses and may reduce radiances to below the camera's threshold. A different method was sought to accurately measure the net radiometric or photometric transmission or reflection by a sample across wavebands of interest, such as segments of the visible and NIR.

The approach is to break up the spectrum into wavebands over which the camera's sensitivity is reasonably flat. Ideally, box-like filters could sample the spectrum over intervals defined by each channel's spectral sensitivity. These could be defined so that if the average sensitivity over the band was used to predict radiance, the measured radiance would differ from the true radiance by no more than a defined value, such as 20 percent. For 20 percent accuracy, this would require 32 filters from 380 to 945 nm, with some bands as large as 725 to 810 nm and many as small as 5 nm. However, real filters are not available or affordable at arbitrary cutoffs with box-like features. In addition, the device need not measure monochromatic radiances, but rather spectral radiances likely to emerge from complex fenestration systems.

To study the potential for accurate radiance measurements across even larger wavebands but flatter spectra, simulations of the cameras output were conducted for a variety of filter combinations. The filters investigated included many combinations of Schott shortpass, longpass, and bandpass

color glass filters. Knowing the spectral properties of the filters and all elements of the goniophotometer, the absolute responsivity of the camera to light from a sample that is spectrally neutral across the filterband is given by (for transmission measurements):

$$\left[\frac{1}{h^{0.3}_{R,G,B,filterband}}\right]_{neutral} = \sum_{filterband} \frac{a_{\Delta\lambda,band}}{h^{0.3}_{R,G,B,\Delta\lambda}}$$

$$a_{\Delta\lambda,band} = \frac{p_{\Delta\lambda,Dedolight}\,\tau_{\Delta\lambda,Filter}\,\rho_{\Delta\lambda,Ellipsoid}}{\sum_{filterband} p_{\Delta\lambda,Dedolight}\,\tau_{\Delta\lambda,Filter}\,\rho_{\Delta\lambda,Ellipsoid}}$$

Using this responsivity, the radiance of the filtered beam can be estimated to a level of accuracy that depends on the spectral transmissivity or reflectivity within each band. By comparing this predicted radiance to the radiance impinging on the sample, the average reflectivity across the filter band can be calculated. By using many filters that together span the entire 380-945 nm range, banded, spectral radiometric and photometric BT(R)DF can be constructed from the BT(R)DF estimates of each filter band.

For samples that have spectrally neutral transmissivity or reflectivity across a filterband, the radiance within the band will be predicted to within the calibration errors for each channel, about 9 percent for R and 5 percent for G and B. For samples that are not neutral within the band, additional error is introduced. The errors introduced for spectral samples depend on the filters chosen and are explained in the section that follows. Only in extreme cases, not likely to be encountered by the device, are errors unacceptable. For example, narrow passband filters or systems with many large, step-like transitions cannot be analyzed reliably, but that is not the intended use of the device.

The filters selected are shown in Table 1 and the resulting filtered HMI spectra are shown in Figure 8. These filters span many wavelengths where either the R, G, or B channel have gradually changing ASR, and span fewer wavelengths where the channel ASR have greater slopes. There are also more filters for wavelengths at which the photopic response curve has the greatest slope. For the variety of materials studied, these filters predicted total radiance from 380 to 945 nm to within 5 percent or less, and in most cases to within 2 percent. For gradually changing spectral reflectivities, the error was found to be very small, less than 1 percent. The total photometric errors were similar, less than 2 percent for most samples but as high as 6 percent for one. The sample that showed 5 percent error in radiometric BRDF over 380-945 nm and 6 percent error in photometric BRDF was a sample with very low reflection coefficients and small BRDF, such that any errors were significant relative to the total.

TABLE 1: FILTER SPECIFICATIONS

APPROXIMATE WAVEBAND	SCHOTT COLOR GLASS FILTERS AND THICKNESSES
1) 380-500 nm	GG400 (1 mm), BG25 (2 mm), BG39 (1mm)
2) 450-590 nm	GG455 (2 mm), BG7 (2 mm)
3) 480-590 nm	GG495 (2 mm), BG 7 (2 mm)
4) 500-650 nm	OG530 (2 mm), BG42 (2 mm)
5) 550-640 nm	OG570 (2 mm), BG39 (2 mm)
6) 570-690 nm	OG590 (2 mm), BG40 (2 mm)
7) 650-850 nm	RG665 (2 mm), KG1 (2 mm)
8) 800-945 nm	RG830 (2 mm)

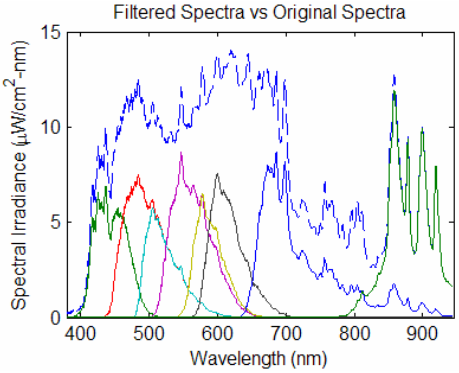

Fig. 8: Original spectra of the HMI lamp and filtered spectra

Within each band, the error in predicted versus real radiance was also generally less than 5 percent for the real samples studies. However, for some samples, especially those with rapidly changing spectral properties within the waveband, errors as high as 12 and in one case for one band, 30 percent were observed. Hypothetical samples that had linearly changing spectral reflectivity or transmissivity from 0 to 1 across each band produced errors in predicted radiance that were less than 8 percent for bands 3 and 6, 20 percent for bands 1, 7 and 8, 25 percent for bands 2 and 4, and 28 percent for band 5. However, most samples studied by the spectral video-goniophotometer will not show the exotic spectral properties that led to the these errors.

For one of the real samples simulated, Figure 9 shows the spectral reflection coefficients for a given direction predicted by the camera along with the real reflection coefficients of the sample. This is a typical example of the banded, spectral reflection coefficients predicted by the simulated video-goniophotometer. The fine resolution of the spectral reflectivity is lost, particularly over the large wavebands, such as the 650-825 nm band. The errors in radiance over each band generated by this sample are less than 2.5 percent above calibration errors for all bands except band 7, for which the additional error is 10 percent. However, the error in predicted total radiance and

luminance from 380-945 nm is only 2.3 and 1.7 percent above calibration errors.

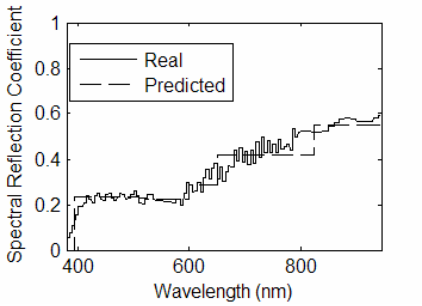

Fig. 9: Real vs predicted reflection coefficients

Although a more detailed analysis of banded, spectral BT(R)DF error will be performed once the filters are acquired, the simulations show that, in addition to the calibration error for each channel, total radiometric BT(R)DF across 380 to 945 nm and total photometric BT(R)DF can be estimated to within about 5 percent for the spectrally and angularly selective fenestrations likely to be studied. The average BT(R)DF within each spectral band will depend on the sample studied, but for a variety of real samples simulated were less than 5 percent. Other aspects of the goniophotometer, such as the spectral properties of the ellipsoid, will introduce additional error in these measurements and will be measured once the goniophotometer is complete.

6. CONCLUSIONS

The method for calculating banded, spectral radiometric and photometric BT(R)DF described above provides an innovative approach to measuring the spectral bi-directional properties of advanced fenestration systems using digital imaging techniques. The spectral, video-goniophotometer at MIT, which is near completion, will be able to estimate photometric BT(R)DF, radiometric BT(R)DF from 380 to 1700 nm (including the NIR camera), and banded, spectral radiometric BT(R)DF to within reasonable accuracies. The typical camera calibration errors are about 5 and 9 percent, depending on the camera channel, and the errors introduced by the banded, BT(R)DF estimation method are generally less than 5 percent. The total error will be validated once the goniophotometer is complete. These innovative capabilities for a video-goniophotometer will enable new and faster analysis of the angular and spectral optical properties of fenestration systems relevant to thermal and daylighting performance.

6. ACKNOWLEDGMENTS

This material is based upon work jointly supported by the Massachusetts Institute of Technology and by the National Science Foundation under Grant No. 0533269. The authors wish to thank Eleanor Stokes for her diligent work researching and selecting absorption filters and Courtney Phillips, Dean Ljubicic, Zachary Clifford, Timothy Koch, and Roselin Osser for their contributions to the device.

5. REFERENCES

(1) "2006 Buildings Energy Databook", http://buildings databook.eren.doe.gov/docs/1.1.3.pdf (accessed 4-13-07), September 2006, U.S. Department of Energy

(2) M. Kischkoweit-Lopin. "An Overview of Daylighting Systems", Solar Energy Vol. 73 No. 2, pp. 77-82, 2002.

(3) H. Koster. Dynamic Daylighting Architecture: Basics, Systems, Projects. August 1, 2004, Birkhauser

(4) R. Sullivan, L. Beltran, E.S. Lee, M. Rubin, and S.E. Selkowitz. "Energy and Daylight Performance of Angular Selective Glazings", *Proceedings of the ASHRAE/DOE/ BTECC Conference,* December 7-11 1998

(5) M. Andersen, J. de Boer. "Goniophotometry and assessment of bidirectional photometric properties of complex fenestration systems", Energy and Buildings 38 (2006) 836-848

(6) G.J. Ward, "Measuring and modeling anisotropic reflection", ACM SIGGRAPH Comput Graphics 26 (2) (1992) 265-272

(7) P. Apian-Bennewitz. "pab Gonio-Photometer II", http://www.pab-opto.de/gonio-photometer/ (accessed 4-14-07), 2007, pab-opto consultancy

(8) M. Andersen, C. Roecker, J.L. Scartezzini. "Design of a time-efficient video-goniophotometer combining bidirectional functions assessment for transmission and reflection", Solar Energy Materials and Solar Cells 88 (2005) 97-118

(9) C. Browne. "Development of a light detection system for bidirectional measurements over the solar spectrum and sun course simulations with Scale Models", June 5, 2006. Massachusetts Institute of Technology

(10) M. Andersen, D. Ljubicic, C. Browne, S. Kleindienst, M. Culpepper. "Automated Assessment of Light Redirecting Properties of Materials and Sunlight Penetration within Scale Models: The Heliodome Project". *Proceedings of the ISES 2005 Solar World Congress*, August 8-12, 2005

(11) G. Holst. CCD arrays, cameras and displays, 1998, SPIE Optical Engineering.

(12) F. Martinez-Verdu, J. Pujol, A. Bouzada, and P. Capilla. "Spectroradiometric characterization of the spectral linearity of a conventional digital camera", *IS&T/SPIE Conference on Color Imaging, January 1999*. International Society for Optical Engineering

(13) S. Brown, T. Larason, C. Habauzit, G. P. Eppeldauer, Y Ohno, K. Lykke. "Absolute Radiometric Calibration of Digital Imaging Systems", *Proceedings of SPIE* Vol. 4306 (2001). International Society for Optical Engineering